

# Phonons of (100) and (110) iron surfaces from first-principles calculations

J. Łażewski,<sup>1,\*</sup> J. Korecki,<sup>2,3</sup> and K. Parlinski<sup>1</sup>

<sup>1</sup>*Institute of Nuclear Physics Polish Academy of Sciences, Radzikowskiego 152, 31-342 Kraków, Poland*

<sup>2</sup>*Institute of Catalysis and Surface Chemistry Polish Academy of Sciences, Niezapominajek, 30-239 Kraków, Poland*

<sup>3</sup>*Faculty of Physics and Applied Computer Science, University of Science and Technology, Mickiewicza 30, 30-059 Kraków, Poland*

(Received 23 October 2006; revised manuscript received 12 December 2006; published 6 February 2007)

Using the density functional theory and the direct method, phonon dispersion relations and phonon density spectra have been calculated for two slabs with Fe(100) and Fe(110) surfaces. A drastic difference between phonon state distributions for both surfaces has been found. The magnetic moments of surface Fe atoms are enhanced by 30% and 14% for (100) and (110) surfaces, respectively.

DOI: [10.1103/PhysRevB.75.054303](https://doi.org/10.1103/PhysRevB.75.054303)

PACS number(s): 68.35.Ja, 31.15.Ar, 63.20.Dj

## I. INTRODUCTION

Surface phonons are a subject of many contributions in the last few decades and are one of the highly interesting effects studied at the surface. The study of elastic surface waves has a very long history. It started in 1885 from Lord Rayleigh's work *On waves propagated along the plane surface of an elastic solid*,<sup>1</sup> which initiated the theory of solitons. In 1911, Augustus Love mathematically predicted the existence of so called *Q waves*,<sup>2</sup> which appear on the surface of a macroscopic layer deposited on a substrate of another material. In seismology, Love waves are the surface seismic waves, which cause horizontal vibrations of the earth during earthquakes. The general formulation of the vibrational properties of systems with two-dimensional periodicity was given by Allen *et al.*<sup>3</sup> The same authors also studied the vibrational surface modes for monoatomic fcc crystals.<sup>4</sup>

Complete and accurate information on phonon spectra and on the interatomic coupling can be obtained from *ab initio* calculations. The reliable calculation of surface mode eigenvectors further opens the way for the more accurate simulation of inelastic scattering intensities, which is pertinent for a proper interpretation of experimental spectra. *Ab initio* calculations of dynamical properties of metal surfaces are discussed in the recent review paper by Heid and Bohnen.<sup>5</sup> They collected and discussed a wide variety of computational results reported earlier. However, no calculations of phonons for magnetic surfaces are mentioned there. On the other hand, surface magnetism is an important subject not only from a fundamental point of view but also for technical applications such as the magneto-optic information-storage devices.<sup>6</sup>

Surface phonons can be measured using helium atom scattering (HAS) and electron-energy-loss spectroscopy. HAS technique was used to investigate the effect of surface magnetization on the surface phonons of Fe(110).<sup>7</sup> Nuclear inelastic scattering (NIS) of synchrotron radiation is a powerful experimental method to study vibrational properties. Recently, it has been shown<sup>8</sup> that for <sup>57</sup>Fe the method could have monolayer sensitivity and can be applied for studying surface and near surface phonons. NIS gives phonon density spectra from a model-free approach. Thus, it can be directly compared with theoretical data. This feature motivates us to undertake extensive calculations of vibrational properties at surfaces.

The aim of this work was to predict phonon dispersion relations and phonon density spectra for (100) and (110) bcc iron surfaces. Fe(110), as the closest-packed surface of the bcc structure, is basically bulk-terminated, with very little atomic relaxation and no reconstruction. On the other hand, the Fe(100) surface is much more open and considerably less stable than Fe(110). In this paper, we compare dynamical properties of both surfaces with respect to their stability. We also discuss the changes of magnetic moment across a slab from its surface towards the center. The paper starts from the description of the calculation method in Sec. II. Then, in Sec. III, obtained results are discussed. Finally, in Sec. IV, we draw some conclusions and outline some perspectives for the future.

## II. CALCULATION SETUP

We have performed first-principles calculations based on spin-polarized density functional theory<sup>9</sup> as implemented in the Vienna *ab initio* simulation package (VASP).<sup>10</sup> It solves the Kohn-Sham equations with periodic boundary conditions and a plane-wave basis set. In the present calculations, Blöchl's all-electron projector augmented wave method<sup>11,12</sup> has been employed. For the treatment of electron exchange and correlation, we used the generalized gradient approximation of Perdew-Burke-Ernzerhof.<sup>13</sup> Brillouin zone integrations were done over a  $4 \times 4 \times 2$  *k*-point mesh generated with the Monkhorst-Pack scheme.<sup>14</sup> The first order Methfessel-Paxton method<sup>15</sup> was used for the Fermi surface smearing, with a width of 0.1 eV. A plane-wave basis set was limited by a kinetic energy cutoff of 350 eV.

The metal surfaces were simulated using a repeated slab geometry. Two slab systems with (100) and (110) orientations, referred to as S100 and S110, were considered. They consisted of seven and five atomic layers of metal atoms in the slab, respectively. We used different numbers of layers to have similar thicknesses of both slabs. The vacuum separation was chosen to be 10% thicker than the respective slab to remove any interaction between surfaces through the vacuum in the periodic boundary conditions.<sup>16</sup> All calculations were done in  $2 \times 2 \times 1$  supercells with 28 and 40 atoms for S100 and S110, respectively. In the course of structural relaxation, all atomic positions and lattice spacings were optimized. A number of electronic steps were carried out until the total

TABLE I. A comparison of calculated in-plane lattice constants ( $a$ ,  $b$ ), interlayer spacings ( $d_{ij}$ ), as well as magnetic moments at the surfaces ( $\mu_s$ ) and at the central layers ( $\mu_c$ ) with the previous slab calculations (Refs. 22 and 23) and the experimental data for bcc iron (Ref. 17). The values of inner spacings ( $d_{23}$  and  $d_{34}$ ) correspond well to 1.434Å and 2.028Å of bulk bcc along the (100) and (110) directions, respectively.

	Fe(100)			Fe(110)		Bulk
	S100	Ref. 22	Ref. 23	S110	Ref. 23	Ref. 17
$a$ (Å)	2.793	2.708	2.863	2.782	2.863	2.867
$b$ (Å)				4.005		4.056
$d_{12}$ (Å)	1.43		1.39	2.02	2.02	
$d_{23}$ (Å)	1.49		1.46	2.03	2.04	
$d_{34}$ (Å)	1.45		1.48		2.04	
$\mu_s$ ( $\mu_B$ )	2.98	2.98	3.05	2.59	2.74	
$\mu_c$ ( $\mu_B$ )	2.28	2.25	2.65	2.28	2.54	2.22

energy difference in subsequent steps was less than  $10^{-8}$  eV. The ionic step optimization was continued until the residual force components of unconstrained atoms were within  $10^{-5}$  eV/Å.

### III. RESULTS AND DISCUSSION

#### A. Crystal structure and magnetic moments

In the bcc structure, each atom has eight nearest-neighbors (NNs) at a distance of  $a_b\sqrt{3}/2$ , and six next-nearest-neighbors (NNNs) at  $a_b$ , where  $a_b$  is the crystallographic lattice constant of bcc structure. However, surface atoms on Fe(100) and Fe(110) are coordinated in different ways. Atoms of the (100) surface are missing four NNs and one NNN, whereas those of the (110) surface do not have two NNs and two NNNs. This fact results in different surface relaxations, reflected in the first interlayer spacing ( $d_{12}$ ), as well as in different increases of surface magnetic moments. Taking into account geometrical aspects only, one should expect larger changes of  $d_{12}$  spacing and higher magnetic moments ( $\mu_s$ ) at the (100) surface than at the (110) one.

After optimization, we obtained equilibrium lattice constants and local magnetic moments listed in Table I. One can see that the calculated in-plane lattice spacings are slightly smaller than the experimental bcc bulk values<sup>17</sup> (about 3%). They are also shorter than those obtained with a different setup in the previous calculations.<sup>23</sup> However, one should take into account that for the phonon study, the whole system must be fully relaxed (not only the outer most layers). On the other hand, the obtained interlayer spacings in the slab center fit the bulk ones much better. The visible disagreement between different directions originates mainly from the elongated supercell shape and was also observed for other compounds.<sup>18,19</sup> Optimized NN distances are quite similar for both surfaces. As expected, a negligible difference in the first two interlayer spacings  $d_{12}$ - $d_{23}$  for S110 and a significantly higher one for S100 were obtained. It is in agreement with previous *ab initio* calculations<sup>20,21</sup> which point out the existence of a deep (up to the third layer) modification of interlayer distances for the Fe(100) surface, with significant

oscillation around the bulk spacing. Both systems are ferromagnetically ordered, with identical magnetic moments at the central layer ( $\mu_c$ ) and higher magnetic moment at the Fe(100) surface ( $\mu_s$ ). The same behavior was observed in the previous *ab initio* calculations.<sup>22,23</sup>

#### B. Phonons

The zone-center optical phonon mode frequencies, phonon dispersion curves, and phonon density of states were calculated using the direct method,<sup>24,25</sup> which has been previously successfully applied to calculate the vibrational properties of several other compounds with different structures (see, e.g., Refs. 18, 26, and 27). The considered unit cells contain seven (S100) and five (S110) nonequivalent atoms, which give rise to 21 and 15 phonon branches, respectively. Since our systems are described by different symmetry

TABLE II. A comparison of calculated optical phonon mode frequencies (in THz) at the  $\Gamma$ -point of the Brillouin zones for slabs terminated with (100) and (110) surfaces.

S100		S110	
Mode	Frequencies	Mode	Frequencies
$A_{2u}, E_u$	0.000	$B_{1u}, B_{2u}, B_{3u}$	0.000
$E_g$	1.509	$B_{3g}$	1.317
$A_{1g}$	2.240	$B_{2g}$	1.607
$E_u$	3.318	$A_g$	2.699
$E_g$	4.567	$B_{2u}$	2.819
$A_{2u}$	4.738	$B_{3u}$	3.323
$E_u$	5.751	$B_{3g}$	4.060
$A_{1g}$	6.579	$B_{2g}$	4.777
$E_g$	6.805	$B_{2u}$	4.890
$A_{2u}$	7.682	$B_{1u}$	5.757
$E_u$	8.017	$B_{3u}$	6.010
$A_{1g}$	8.308	$A_g$	7.843
$A_{2u}$	8.829	$B_{1u}$	9.164

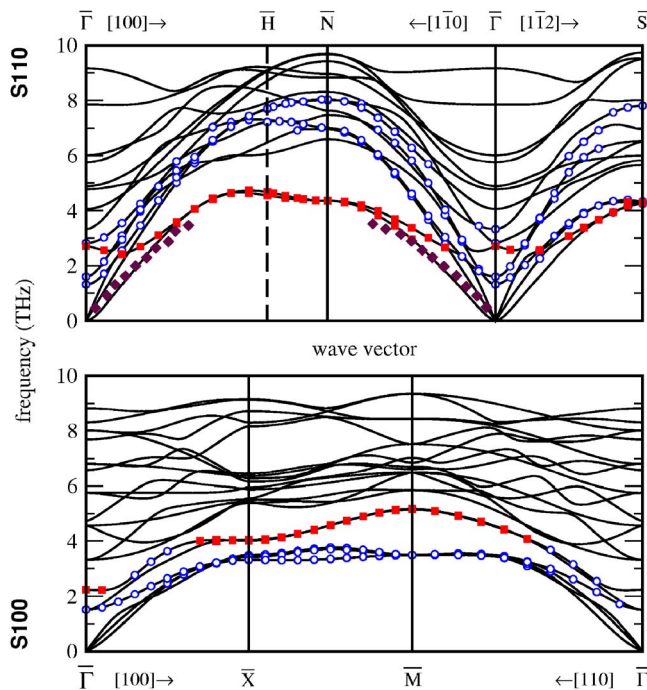


FIG. 1. (Color online) Calculated phonon dispersion curves for S110 and S100 slabs, terminated with the (110) and (100) bcc Fe surfaces, respectively. The open circles and filled squares denote the highest intensity surface modes with polarization along the in-plane and out-of-plane directions, respectively. Experimental points depicted by diamonds refer to HAS measurements taken at 150 K (Ref. 7).

groups (tetragonal  $P4/mmm$  for S100; orthorhombic  $Cmmm$  for S110), the  $\Gamma$ -point phonon modes decompose at the appropriate Brillouin zones according to different sets of irreducible representations. The phonon frequencies at the Brillouin zone centers for both systems are listed in Table II. All modes are optically active: *gerade* modes are Raman active, whereas *ungerade* modes are infrared active.

In Fig. 1, the calculated phonon dispersion curves along several selected directions of the surface Brillouin zones are shown. In the presentation, we used plane reciprocal lattices defined by Allen *et al.*<sup>3</sup> Following their notation, all high symmetry points of a two-dimensional Brillouin zone were labeled by barred letters to distinguish them from points in a three-dimensional zone. Simulated structures are dynamically stable without any soft-mode behavior. Also for both slabs, the calculated phonon relations perpendicular to the surface were flat, which confirms that there is no interaction among the neighboring slabs across the vacuum. The intervals of phonon frequencies in both spectra are similar. However, for S110, these intervals reach slightly higher frequencies. Taking into account the polarization vectors for a particular atom, one can obtain its contribution to respective phonon modes.<sup>25</sup> In Fig. 1, we distinguished phonon branches with the highest contribution of surface atom vibrations. To differentiate in-plane and out-of-plane components, we used open circle and filled square symbols, respectively. For S110, we obtained lower frequencies for vibrations perpendicular to the surface, traditionally called Rayleigh's wave (RW). However, for S100, the order is op-

posite and the lowest state is occupied by an in-plane component just below RW. We believe that it is associated with an inward relaxation of the surface layer that is significantly higher than in the Fe(110) case. In most cases, the RW corresponds to the lowest surface mode. However, in some particular systems, the lowest mode is shear horizontally polarized. It was observed, for instance, by Allen *et al.* for the (100) surface in cubic fcc crystals.<sup>4</sup> In Fig. 1, we also put HAS data taken for Fe(110) at 150 K.<sup>7</sup> One can see that our results correspond very well to the experimental data. Moreover, from the temperature dependence of the RW frequencies presented there, one can expect that at  $T=0$  K, the agreement should be even better.

The in-plane phonon densities of states are presented layer by layer in Fig. 2. Upper lines for both systems illustrate surface phonon states. Both of the central layer contributions—especially that for S110—resemble the total phonon density of states (DOS) of bulk bcc iron<sup>28</sup> in their shape denoted with the filled contour. However, at first sight, one can see that the main difference between both spectra is in the shape and position of the contribution of surface phonons. For the (100) surface, phonon states compose a peak at about 3.3 THz completely separated from others, while those for (110) spread out nearly in the whole interval of the spectrum. The origin of this significant difference could be traced back to the neighborhood of the surface atoms and to the loss of bulk NNs and NNNs. Indeed, in the (110) surface, each Fe atom has four neighbors at  $a_b\sqrt{3}/2$ , whereas on the Fe(100) surface, each atom also has four neighbors but at the  $a_b$  distance. Additionally, atoms in the (100) surface are missing four NNs and one NNN, while atoms in the (110) surface two NNs and two NNNs, which causes the atoms on the (110) surface to be more strongly

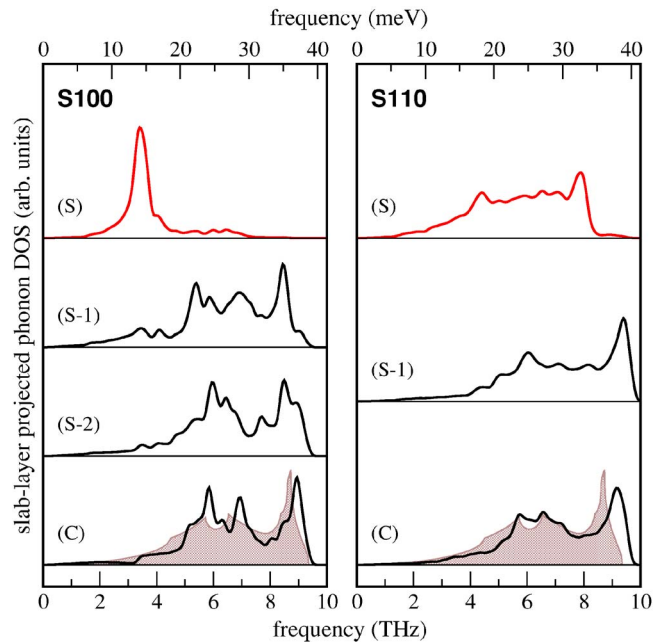


FIG. 2. (Color online) Calculated in-plane layer-projected phonon densities of states for surface (S), subsurface (S-1, S-2), and central (C) atomic layers. Filled shapes correspond to experimental phonon DOS taken from Ref. 28.

bound. As a consequence, they have higher vibration frequencies than those on the (100) surface.

#### IV. CONCLUSIONS

We have optimized two slabs of bcc iron with (100) and (110) surfaces. In both cases, we obtained good agreement with lattice spacings and magnetic moments measured in experiments. Calculated phonon dispersion curves confirm the stability of both surfaces. However, in the (100) case, the mean phonon frequency is lower. It indicates—in accordance with the general knowledge—that the (110) surface is more stable than the (100) one. Comparing the layer-projected phonon density of states, we found localized surface modes

for the (100) surface and a rather broad distribution of frequencies for the (110) surface. We believe that the presented *ab initio* results can be verified experimentally, for example, by the nuclear inelastic scattering measurements.

#### ACKNOWLEDGMENTS

The authors thank P. Piekarczyk and P. T. Jochym for fruitful discussions and assistance in the calculations. This work was partially supported by the European Community under FP6 Contract No. NMP4-CT-2003-001516 (DYNASYNC). J. Ł. acknowledges support by the Polish Ministry of Science and Education under Project No. 1 P03B 104 26. Calculations have been partially performed in the ACK Cyfronet AGH, computational Grant No. MNiSW/SGI2800/IFJ/129/2006.

\*Electronic address: jan.lazewski@ifj.edu.pl

<sup>1</sup>L. Rayleigh (J. W. Strutt), Proc. London Math. Soc. **17**, 4 (1885).  
<sup>2</sup>A. E. H. Love, *Some Problems of Geodynamics* (Cambridge University Press, London, England, 1911).  
<sup>3</sup>R. E. Allen, G. P. Alldredge, and F. W. de Wette, Phys. Rev. B **4**, 1648 (1971).  
<sup>4</sup>R. E. Allen, G. P. Alldredge, and F. W. de Wette, Phys. Rev. B **4**, 1661 (1971).  
<sup>5</sup>R. Heid and K.-P. Bohnen, Phys. Rep. **387**, 151 (2003).  
<sup>6</sup>S. D. Bader and C. Liu, J. Vac. Sci. Technol. A **9**, 1924 (1991).  
<sup>7</sup>G. Benedek, J. P. Toennies, and G. Zhang, Phys. Rev. Lett. **68**, 2644 (1992).  
<sup>8</sup>R. Röhlberger, A. I. Chumakov, P. T. Jochym, J. Korecki, J. Łazewski, K. Parlinski, R. Rüffer, B. Sepiol, M. Sladeczek, T. Ślęzak, N. Spiridis, S. Stankov, and G. Vogl (unpublished).  
<sup>9</sup>P. Hohenberg and W. Kohn, Phys. Rev. **136**, B864 (1964); W. Kohn and L. J. Sham, Phys. Rev. **140**, 1133 (1965).  
<sup>10</sup>G. Kresse and J. Furthmüller, Phys. Rev. B **54**, 11169 (1996); G. Kresse and J. Furthmüller, Comput. Mater. Sci. **6**, 15 (1996).  
<sup>11</sup>P. E. Blöchl, Phys. Rev. B **50**, 17953 (1994).  
<sup>12</sup>G. Kresse and D. Joubert, Phys. Rev. B **59**, 1758 (1999).  
<sup>13</sup>J. P. Perdew, K. Burke, and M. Ernzerhof, Phys. Rev. Lett. **77**, 3865 (1996).  
<sup>14</sup>H. J. Monkhorst and J. D. Pack, Phys. Rev. B **13**, 5188 (1976).  
<sup>15</sup>M. Methfessel and A. T. Paxton, Phys. Rev. B **40**, 03616 (1989).  
<sup>16</sup>In the phonon calculation, we used the direct method (see Ref. 24) in which interatomic interaction (force constants) range

comprises all neighbors at distances up to half dimensions of the supercell.

<sup>17</sup>*Magnetic Properties of Metals: d-Elements, Alloys and Compounds*, Data in Science and Technology, edited by H. P. J. Wijn (Springer, Berlin, 1991).  
<sup>18</sup>J. Łazewski, K. Parlinski, W. Szuszkiewicz, and B. Hennion, Phys. Rev. B **67**, 094305 (2003).  
<sup>19</sup>J. Łazewski, H. Neumann, and K. Parlinski, Phys. Rev. B **70**, 195206 (2004).  
<sup>20</sup>M. J. S. Spencer, A. Hung, I. K. Snook, and I. Yarovsky, Surf. Sci. **513**, 389 (2002).  
<sup>21</sup>P. Błoński and A. Kiejna, Vacuum **74**, 179 (2004).  
<sup>22</sup>S. Ohnishi, A. J. Freeman, and M. Weinert, Phys. Rev. B **28**, 06741 (1983); S. Ohnishi, M. Weinert, and A. J. Freeman, *ibid.* **30**, 36 (1984).  
<sup>23</sup>P. Błoński, A. Kiejna, and J. Hafner, Surf. Sci. **590**, 88 (2005).  
<sup>24</sup>K. Parlinski, Z. Q. Li, and Y. Kawazoe, Phys. Rev. Lett. **78**, 4063 (1997); K. Kunc and P. Gomes Dacosta, Phys. Rev. B **32**, 2010 (1985); W. Frank, C. Elsasser, and M. Fahnle, Phys. Rev. Lett. **74**, 1791 (1995).  
<sup>25</sup>K. Parlinski, PHONON software, Cracow, Poland, 2005.  
<sup>26</sup>J. Łazewski, H. Neumann, K. Parlinski, G. Lippold, and B. J. Stanbery, Phys. Rev. B **68**, 144108 (2003).  
<sup>27</sup>J. Łazewski, P. T. Jochym, P. Piekarczyk, and K. Parlinski, Phys. Rev. B **70**, 104109 (2004).  
<sup>28</sup>C. Van Dijk and J. Bergsma, *Neutron Inelastic Scattering* (IAEA, Vienna, 1968) Vol. 1, p. 233.